Investigation of Sparse-Build Rapid Tooling by Fused Deposition Modeling

O. Iyibilgin[*], M. C. Leu[**], G. Taylor[**], H. Li[**], and K. Chandrashekhara[**]
[*] Department of Mechanical Engineering, Sakarya University, Sakarya, Turkey
[**] Department of Mechanical and Aerospace Engineering, Missouri University of Science and Technology, Rolla, Missouri, USA

Abstract

This paper describes the investigation of sparse-build tooling by Fused Deposition Modeling (FDM®) aimed at rapid tooling with reduction in the amount of material. Sparse-build test coupons having ULTEM as the material and varying air gap (sparse spacing), wall thickness, and cap thickness were fabricated using the sparse and sparse-double dense build styles of the Stratasys Fortus machine. The strengths and moduli of these coupons were measured in compression and flexure tests. The strength/mass ratio and modulus/mass ratio were compared among the various coupons, as well as with solid coupons, to investigate the effects of the two build styles and the three sparse-build parameters. In addition, the effects of build direction and raster orientation were also studied.

1. Introduction

Additive manufacturing (AM) technology holds great promise for many applications and is currently growing at an extraordinary speed. As defined by ASTM F42 Committee on Additive Manufacturing, AM is "a process of joining materials to make objects from three-dimensional model data, usually layer upon layer, as opposed to subtractive manufacturing methodologies" [1-2]. This process is capable of significant savings of manufacturing cost and lead time in comparison to manufacturing by subtractive processes.

Stratasys Fortus machines can fabricate parts from thermoplastics that are environmentally stable using the Fused Deposition Modeling (FDM) process. The basic materials used in Stratasys Fortus machines include ABS, ULTEM, PC, and PPSF [9-11]. The Fortus machine is capable of fabricating parts using different build styles including solid, sparse, and sparse-double dense. Fabricating parts using the sparse or sparse-double dense build style could significantly reduce the material amount, fabrication time, and energy use. However, it is necessary that the mechanical strength and elastic modulus of the sparse-build parts are still high enough for a given manufacturing application.

The build parameters of AM influence the mechanical properties including strength and modulus of the manufactured parts, which affect the part quality and performance. Substantial research

542

has been conducted by many researchers to investigate the effects of build parameters in the past. Sood et al. [4] demonstrated the importance of build parameters on the part's compressive strength. Iyibilgin et al. [5] conducted experimental tests to evaluate the compressive strength, modulus, and build time for sparse-build parts with different cellular lattice structures fabricated by the FDM process. Montero et al. [6] characterized the effects of raster orientation, air gap, bead width, and environment temperature on the strength of an FDM part. Lee et al. [7] compared the compressive strength of specimens manufactured by FDM versus other AM processes using the same material and amount, and found higher strength in the FDM specimens. Levasseur et al. [8] evaluated the effects of structural parameters on the apparent/effective elastic modulus of FDM bone surrogate parts, and concluded that cortical shell thickness and trabecular bone architecture have significant effect on the bone's modulus.

In the current study ULTEM 9085 was used as the material due to its high strength and high heat-deflection temperature. This study was aimed at rapid tooling with reduction in the amount of material used. We investigated the effects of different FDM sparse-build parameters on the mechanical properties of ULTEM parts. Both sparse and solid parts were manufactured using a Stratasys Fortus 400mc machine. The sparse parts were fabricated using the sparse and sparse-double dense functions available from the Fortus machine. The build parameters being studied included air gap (sparse spacing), wall thickness, and cap thickness. The mechanical properties including strength and modulus were evaluated using compression and flexural tests. The effects of build direction and raster orientation were also investigated.

2. Experimental Study

Experimental tests were conducted on both solid and sparse-build test coupons fabricated with ULTEM 9085 as the material using a Stratasys Fortus 400 machine. The experimental study was conducted to determine the mechanical properties including strength and modulus in compression and flexure tests. The experimental study was also used to determine the surface quality of the fabricated parts.

2.1. Build Styles and Sparse-Build Parameters

To obtain the yield strength and elastic modulus, stress was plotted against strain for each test coupon in compression and flexure tests. Modulus of elasticity is the slope of the linear portion of the stress versus strain curve. Yield strength is defined as the intersection of the stress-strain curve and a 0.2% offset line with slope equal to the modulus of elasticity.

Cylindrical test coupons having the dimensions of 38.1 mm (1.5") diameter and 25.4 mm (1") length were used in the compression tests. These coupons were fabricated using three build functions: solid, sparse, and sparse-double dense; see Fig. 1. Figure 2 shows the structure of the test coupons fabricated for compression tests. The dimensions of the flexure test coupons were 127 mm length x 25.4 mm width x 6.35 mm height (5" x 1" x 0.25") according to ASTM D790 Standard; see Fig. 3. The sparse-build parameters included air gap, wall thickness and cap

thickness. In total, 27 sets of test coupons with varying combinations of the sparse-build parameters were fabricated for both compression and flexure tests.

2.2. Build Direction and Raster Orientation

Besides the sparse-build parameters, the effects of build direction and raster orientation on mechanical strength and surface roughness were also investigated. To better visualize the effects of build direction and raster orientation on the internal structure of a fabricated part, Figure 4 provides an illustration for two different build directions and two different raster orientations. It helps visualize change in the internal structure of a sparse-build coupon due to variations in build direction and raster orientation. Note that the build direction is always in the vertical up direction, but the applied force may orient differently relative to the build direction. Also, the raster angles may vary as shown in Figure 4 for two sets of raster angles, $(0^o, 90^o)$ and $(45^o, -45^o)$. Figure 5 shows how the different build directions and raster orientations affect the internal structure of the coupon when subjected to an applied force. The applied force may be parallel to the build direction (i.e., normal to the plane of build layer) or perpendicular to the build direction (i.e., parallel to the plane of build layer).

(a)   (b)

(c)
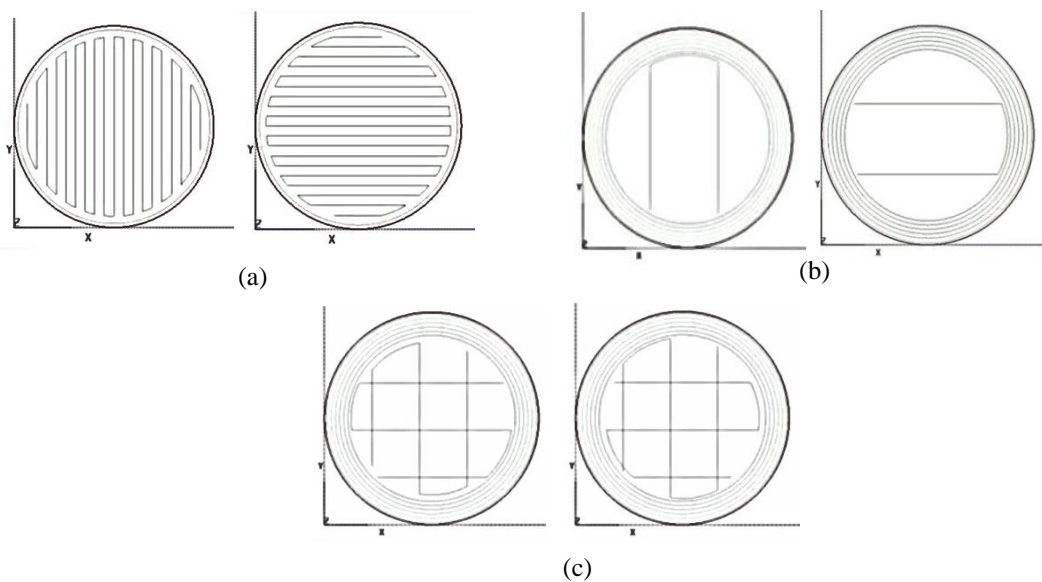
Figure 1 FDM® build styles (a) solid-build, (b) sparse-build, (c) sparse-double dense build.
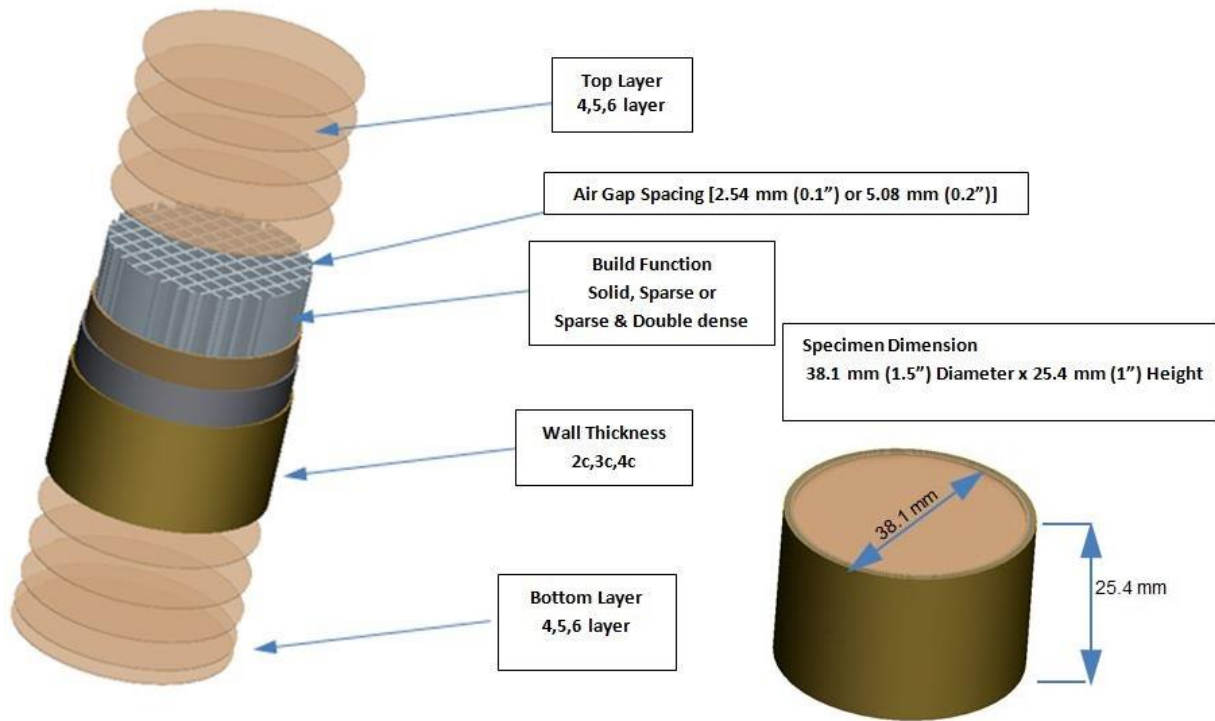
Figure 2 Coupons manufactured using the Fortus 400mc machine for compression tests.
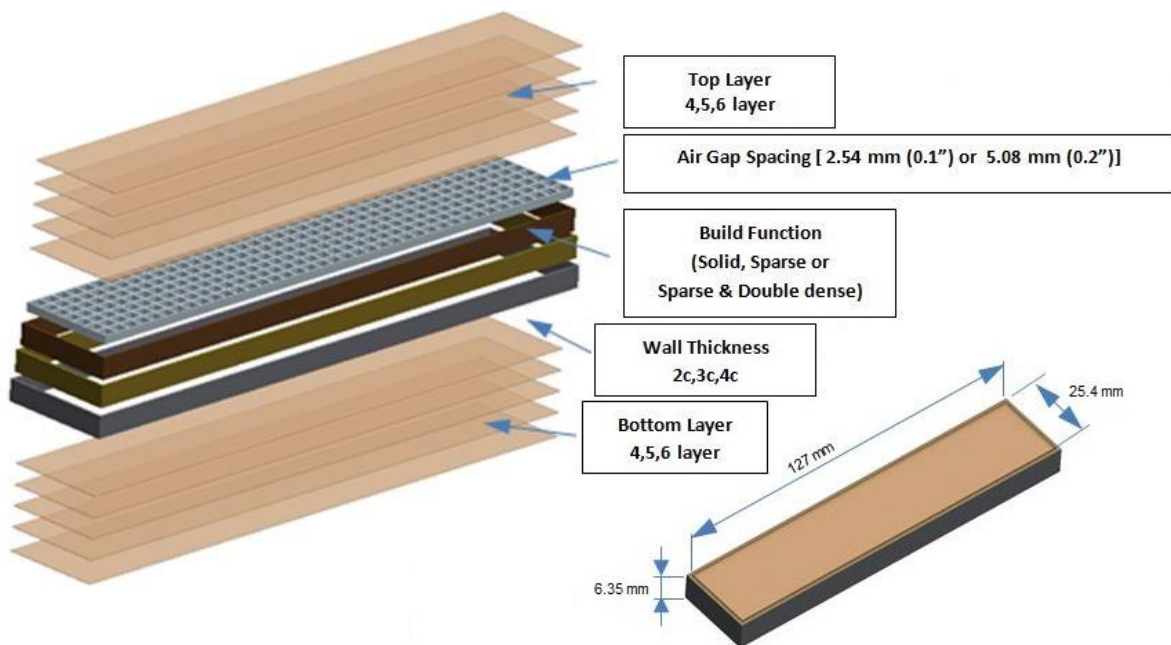
Figure 3 Coupons manufactured using the Fortus 400mc machine for flexure tests.
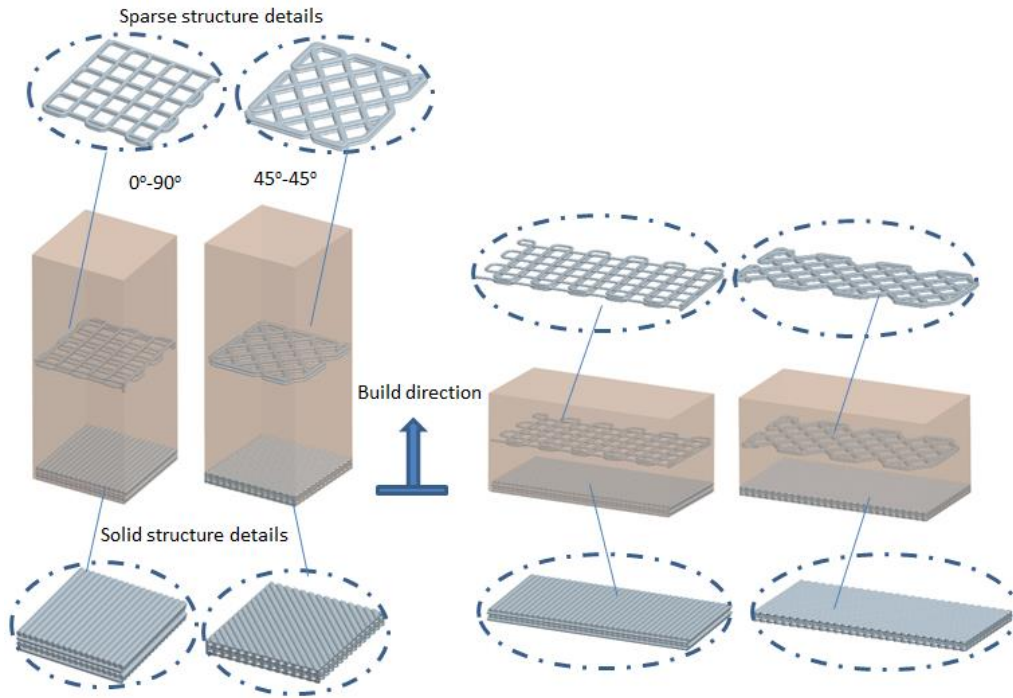
Figure 4 Illustration of different build directions and raster orientations.
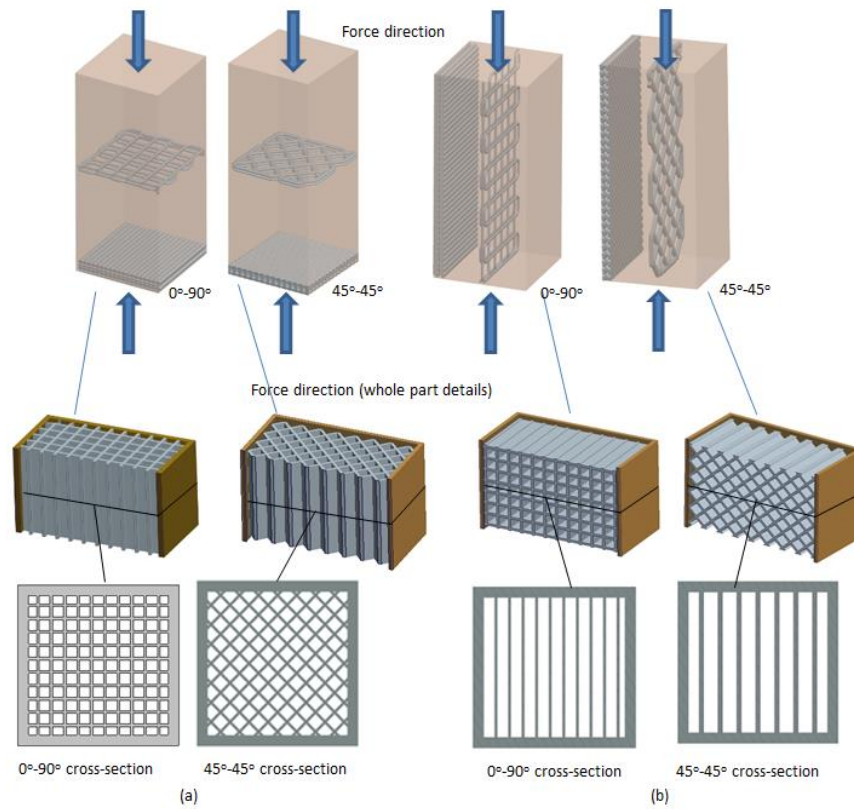
Figure 5 Applied force direction: (a) parallel to the build direction, and (b) perpendicular to the build direction. For each of the two cases, the raster angles may be (0°, 90°) or (45°, -45°).

Three sets of build direction and raster orientation were chosen to investigate their effects on the part's mechanical properties and surface roughness. They are: (1) the applied force is parallel to the build direction, (2) the applied force is perpendicular to the build direction, with the angles between the raster path and the applied force being (0°, 90°), and (3) the applied force is perpendicular to the build direction, with the angles between the raster path and the applied force being (45°, -45°); see Fig. 5. Note that when the applied force is parallel to the build direction, the angles between the raster path and the applied force should have no effect on the mechanical properties; however, when the applied force is perpendicular to the build direction, the angles between the raster path and the applied force should influence mechanical properties. Build direction also has effect on surface roughness. This effect is more pronounced for a curved surface than for a planar surface, thus the effect of build direction on surface roughness was investigated using a curved surface shown in Fig. 6. This figure shows a test specimen with a curved surface and the orientation of this surface with respect to the build direction, which is always in the vertical up direction. The test specimens were built only in the directions of Figure 6 (b) & (c) because the part is much longer in the vertical direction and is likely to deform due to gravity during the fabrication process for the build direction of Figure 6(a).
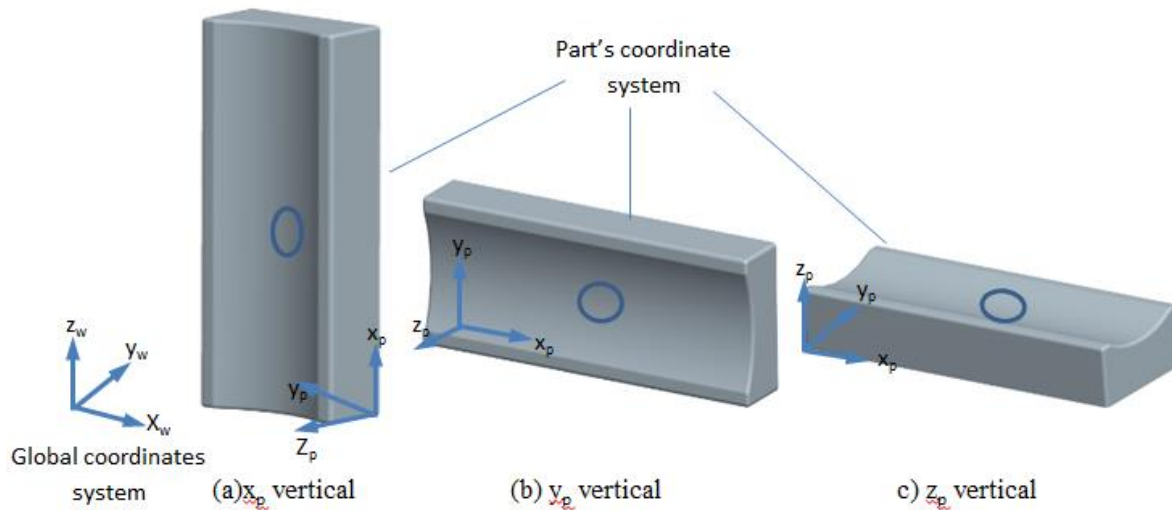
Figure 6 Illustration of different build directions for a test part with a curved surface.

2.3. Test Procedure

Both compression and flexure tests were performed using an INSTRON 4485 test machine with a 200 kN (45,000 lbf) capable load cell. According to ASTM Standards (D695 and D790), 1.27 mm/min (0.05 in/min) and 2.54 mm/min (0.1 in/min) head speeds were used for compression and flexure tests, respectively. Five samples were tested for each set of parameter values with varying air gap, wall thickness, and cap thickness. The tests were performed at room temperature.

3. Results and Discussion

3.1. Effects of Build Style and Sparse-Build Parameters

Table 1 provides the detailed sparse-build parameters and compression test results for coupons fabricated using the sparse and sparse-double dense (SDD) build styles as well as solid-build style. There were 27 sets of sparse-build parameters varying in air gap, wall thickness, and cap thickness. The compression test data obtained were then used to calculate the strength-to-mass ratio and modulus-to-mass ratio averaged over five coupons for each set of parameters. Figures 7 and 8 plot the strength-to-mass ratio and modulus-to-mass ratio for the data given in Table 1. The compressive strength-to-mass ratios of the sparse and sparse-double dense coupons are lower than those of the solid coupon. However, the sparse-double dense coupons have higher compressive modulus-to-mass ratios than the solid coupon.

From the compression test data obtained, it can be seen that air gap is the most important parameter. Test coupons with smaller air gaps clearly have higher strength/mass ratios. Wall thickness also positively affects mechanical properties: as wall thickness increases, the strength/mass ratio increases slightly. Cap thickness has a negative effect on the mechanical properties: increase in cap thickness reduces the strength/mass ratio and modulus/mass ratio. The data from the compression tests with the air gap of 2.54 mm (0.1") and 3.81 mm (0.15") show that the test coupons built with the sparse build (no double dense) style have much lower strength-to-mass and modulus-to-mass ratios compared to the test coupons built with the sparse-double dense build style. For this reason the compression tests for 5.08 mm (0.2") air gap were done for only the sparse-double dense coupons.

Table 2 shows the detailed sparse-build parameters and flexure test results in terms of strength-to-mass ratio and modulus-to-mass ratio for 27 sets of solid, sparse, and sparse-double dense build coupons. Figures 9 and 10 plot the data on strength-to-mass ratio and modulus-to-mass ratio from Table 2. The flexure strength-to-mass and modulus-to-mass ratios of both sparse and sparse-double dense coupons are higher than those of the solid coupon. Since the test coupons with the air gap of 2.54 mm (0.1") and 3.81 mm (0.15") fabricated with the sparse build style have lower strength-to-mass ratios compared to the test coupons with the same air gaps built with the sparse-double dense function, the flexure tests for 5.08 mm (0.2") air gap included only the sparse-double dense coupons. Cap thickness is the most important parameter in the flexure tests. Increase in cap thickness results in increase in the strength/mass ratio and modulus/mass ratio. Air gap also affects the mechanical properties. As air gap increases, both strength/mass ratio and modulus/mass ratio increase slightly. There is no clear trend on the effect of wall thickness.

Table 1 Compression test results for the solid, sparse, and sparse-double dense coupons with different sparse-build parameters

Part #	Air Gap (mm)	Wall Thickness (mm)	Cap Layer Thickness (mm)	Porosity (%)		Strength/mass Ratio (MPa/g)		Modulus/mass Ratio (MPa/g)	
				Sparse	Sdd	Sparse	Sdd	Sparse	Sdd
Solid	-	-	-	-	-	2.61	2.61	30.87	30.87
P1	2.54	1.02	1.02	60.95	45.34	0.75	1.64	23.83	40.13
P2			1.27	59.76	44.22	0.72	1.64	23.08	39.37
P3			1.52	57.99	43.31	0.71	1.62	22.02	38.9
P4		1.52	1.02	57.40	42.34	0.89	1.69	26.42	39.45
P5			1.27	56.21	41.28	0.88	1.65	26.38	39.07
P6			1.52	55.03	40.38	0.85	1.64	25.92	38.71
P7		2.03	1.02	53.85	39.38	1.04	1.68	29.38	38.95
P8			1.27	52.66	38.52	1.01	1.66	28.09	38.81
P9			1.52	51.48	37.59	0.98	1.65	28.09	38.36
P10	3.81	1.02	1.02	68.05	55.35	0.78	1.41	24.71	38.4
P11			1.27	66.27	54.14	0.72	1.39	23.65	37.08
P12			1.52	65.09	52.91	0.70	1.36	22.75	36.52
P13		1.52	1.02	63.91	52.57	0.97	1.42	28.89	38.13
P14			1.27	62.72	51.38	0.93	1.41	27.17	37.32
P15			1.52	60.95	50.25	0.88	1.39	26.75	36.47
P16		2.03	1.02	60.95	49.4	1.06	1.49	31.74	37.91
P17			1.27	59.76	48.28	1.02	1.47	30.54	37.35
P18			1.52	57.99	47.21	0.99	1.44	29.34	36.61
P19	5.08	1.02	1.02		59.48		1.36		39.09
P20			1.27		58.15		1.34		38.25
P21			1.52		56.78		1.33		37.42
P22		1.52	1.02		56.16		1.4		38.34
P23			1.27		54.99		1.36		38.32
P24			1.52		53.82		1.34		37.83
P25		2.03	1.02		53.94		1.53		38.21
P26			1.27		52.81		1.49		38.38
P27			1.52		51.57		1.47		37.66
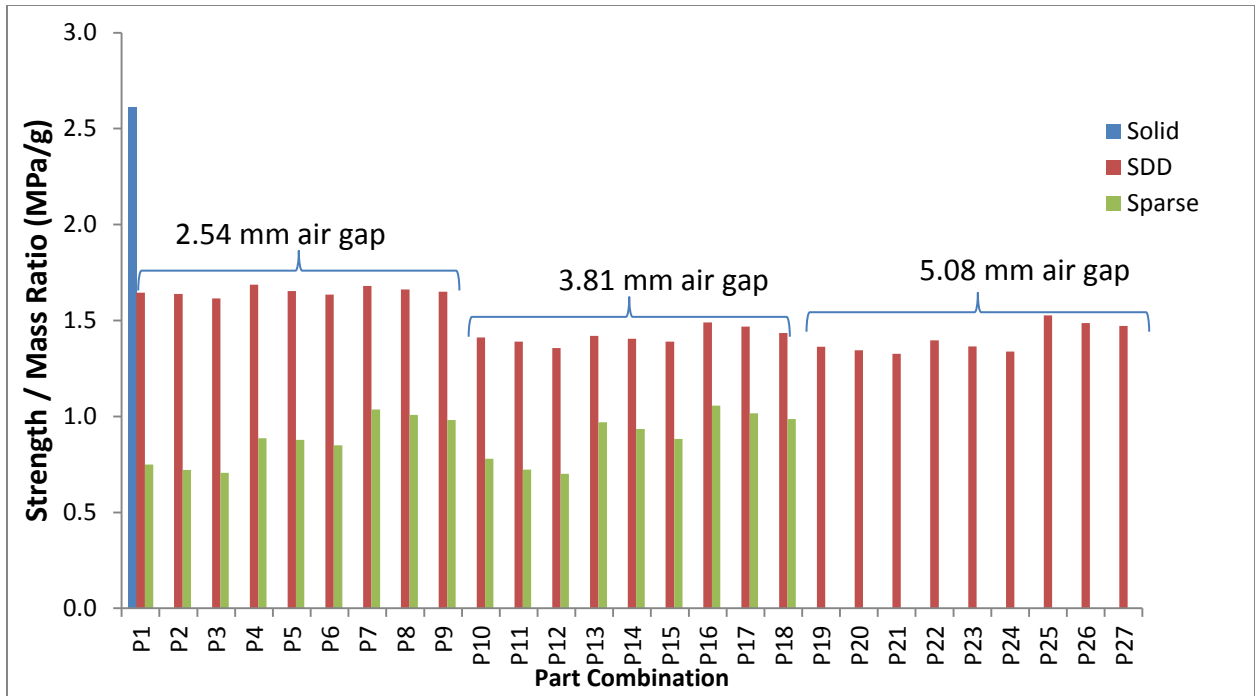
Figure 7 Yield strength/mass ratio comparison for solid, sparse, and sparse-double dense build styles (compression test)
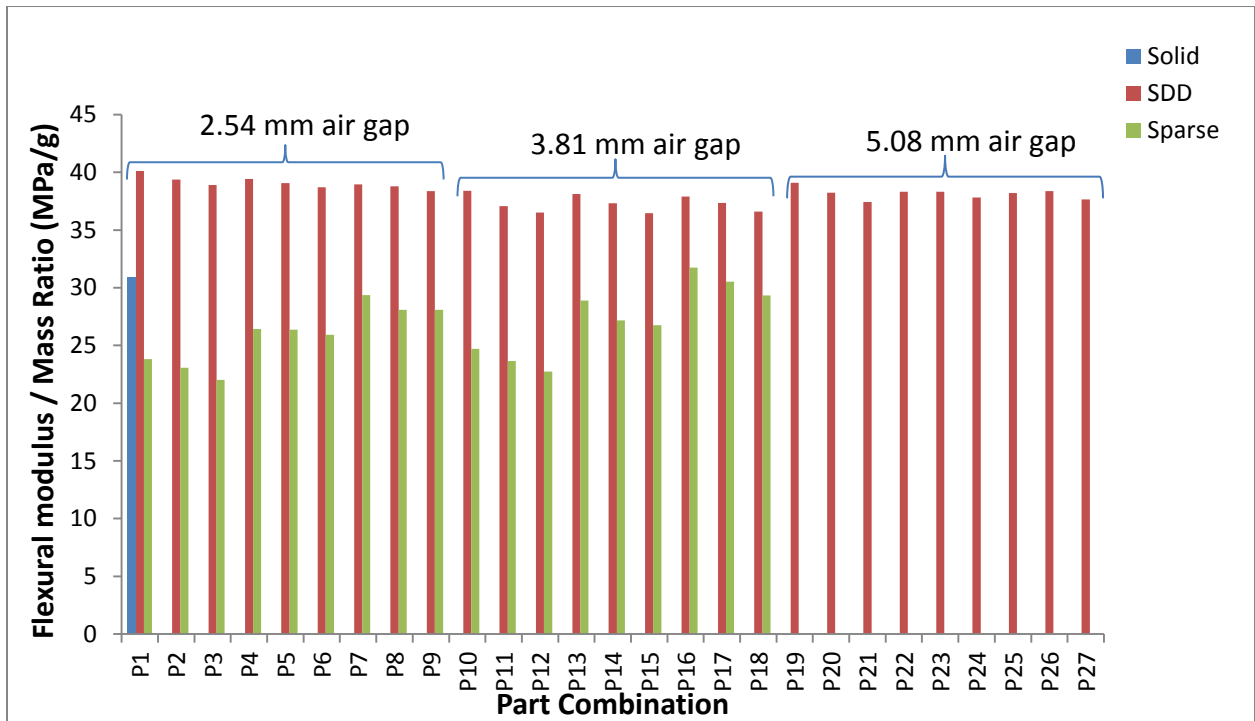
Figure 8 Modulus/mass ratio comparison for solid, sparse, and sparse-double dense build styles (compression test)

Table 2 Flexure test results for the solid, sparse, and sparse-double dense coupons with different sparse-build parameters

Part #	Sparse fill air gap (mm)	Wall thickness (mm)	Cap layer thickness (mm)	Porosity (%)		Strength/mass ratio (MPa/g)		Modulus/mass ratio (MPa/g)	
				Sparse	Sdd	Sparse	Sdd	Sparse	Sdd
Solid	-	-	-		-	2.69	2.69	78	78
P1			1.02	44.53	24	3.13	3.89	89.04	103.12
P2		1.02	1.27	39.06	20	3.25	3.93	93.79	100.67
P3			1.52	33.59	16.8	3.30	4.06	92.10	100.38
P4			1.02	42.19	22.4	3.19	3.99	89.22	100.12
P5	2.54	1.52	1.27	36.72	18.4	3.26	3.96	92.72	100.61
P6			1.52	32.03	15.2	3.25	3.98	91.93	101.81
P7			1.02	39.84	20.8	3.16	4.02	91.89	102.75
P8		2.03	1.27	35.16	17.6	3.20	4.12	92.46	104.03
P9			1.52	30.47	13.6	3.18	4.19	91.49	105.11
P10			1.02	47.66	30.4	3.01	4.17	89.39	106.70
P11		1.02	1.27	42.19	25.6	3.07	4.4	89.97	111.65
P12			1.52	36.72	21.6	2.98	4.58	87.48	16.420
P13			1.02	45.31	28	3.10	4.07	89.71	103.58
P14	3.81	1.52	1.27	39.84	24	3.22	4.45	92.65	110.35
P15			1.52	34.38	20	3.08	4.59	88.67	114.33
P16			1.02	42.97	26.4	3.12	3.99	87.81	99.950
P17		2.03	1.27	37.50	22.4	3.14	4.29	91.88	107.34
P18			1.52	32.81	18.4	3.05	4.42	89.81	108.70
P19			1.02		33.6		4.43		114.32
P20		1.02	1.27		28.8		4.48		115.66
P21			1.52		24		4.33		110.84
P22			1.02		31.2		4.58		115.53
P23	5.08	1.52	1.27		27.2		4.38		108.70
P24			1.52		22.4		4.38		109.15
P25			1.02		29.6		4.3		108.88
P26		2.03	1.27		24.8		4.31		107.20
P27			1.52		20.8		4.31		107.69
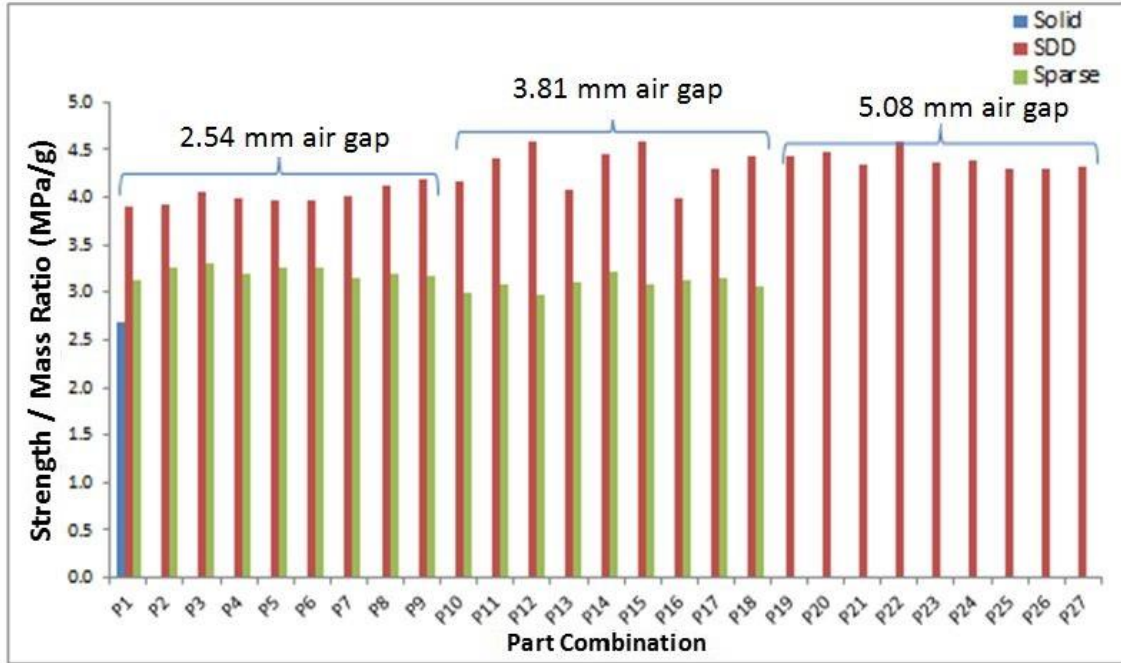
Figure 9 Yield strength/mass ratio comparison for solid, sparse, and sparse-double dense build styles (flexure test)
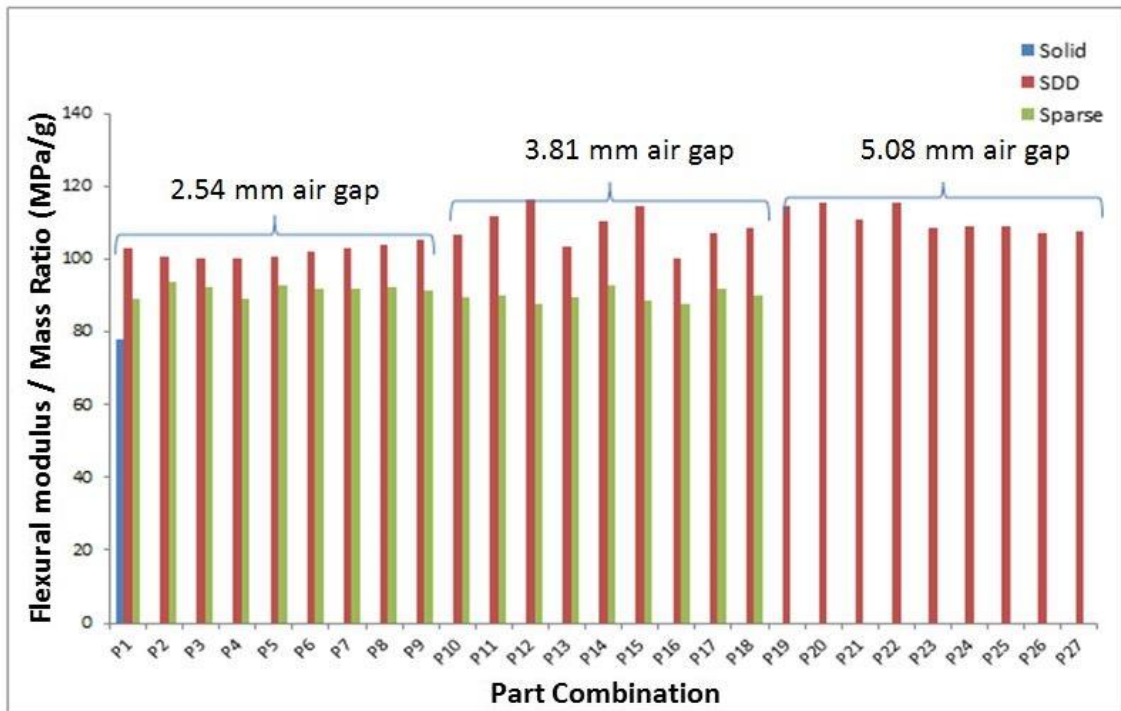
Figure 10 Modulus/mass ratio comparison for solid, sparse, and sparse-double dense build styles (flexure test)

3.2. Effects of Build Direction and Raster Orientation

Table 3 provides the compression test data obtained for coupons fabricated in various build directions and raster orientations. It is clear from the data that the build direction and raster orientation strongly affect the compressive strength and modulus, both of which are significantly higher when the build direction is parallel to the applied force direction than when the build direction is perpendicular to the applied force direction. For the build direction perpendicular to the applied force direction, the strength and modulus are higher when the raster angles are (0°, 90°) compared with the raster angles of (45°, -45°).

In studying the effects of build direction and raster orientation on surface roughness, we first examined the quality of the curved surface generated by different build directions shown in Fig. 6. The photos of these surfaces are shown in Fig. 11. The surface is clearly the smoothest when the build direction is x_p-vertical and is the roughest when the build direction is z_p-vertical. This is because the roughness of a curved surface is mainly due to the stair-step effect, whose severity depends on the angle between the curved surface and the build direction: the smaller the maximum angle between the curved surface and the build direction, the smoother the surface. Because of the likelihood of part deformation in the x_p-vertical build direction, we only compared quantitatively the surface roughness for the y_p-vertical (Figure 6(b)) and z_p-vertical (Figure 6(c)) build directions. The measured surface roughness data are given in terms of R_a (average roughness) and R_m (maximum roughness) in Table 4. The surface roughness is independent of raster orientation, i.e., the surface roughness for the raster angles of (0°, 90°) is the same as the surface roughness for the raster angles of (45°, -45°). Both have the surface that is smooth in the x-direction but relatively rough in the y-direction. In comparison, the surface generated in the z_p-vertical direction is much rougher. Not only the surface's R_a and R_m values were much higher in the x-direction, but its surface roughness in the y-direction was beyond the measurement range of our surface analyzer.

(a) x_p vertical   (b) y_p vertical   (c) z_p vertical
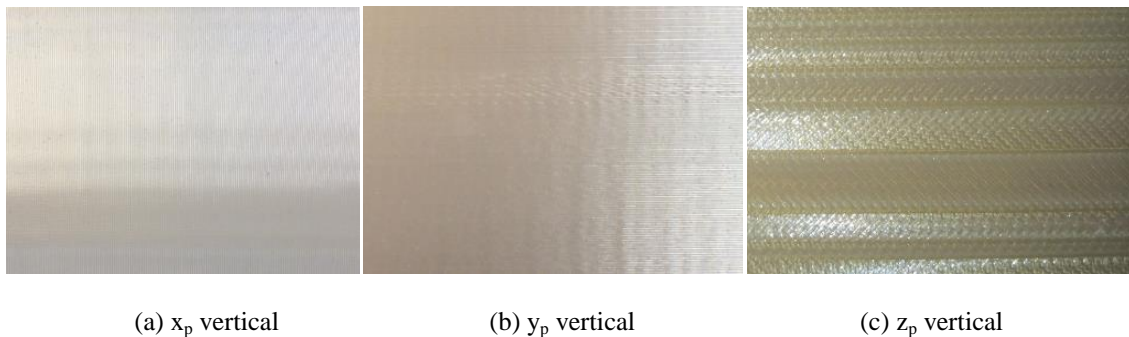
Figure 11. Photographs of the curved surface in Fig. 6 generated in different build directions.

Table 3 Compression test results for coupons fabricated in various build directions and raster orientations

Part #	Air Gap (mm)	Cap and Wall Thickness (mm)	Material Amount ($\times 10^3$ mm^3)	Build Time (min)	Mass (g)	Build Direction Parallel to Applied Force Direction, Raster Angles=(45,-45)		Build Direction Perpendicular to Applied Force Direction, Raster Angles = (0,90)		Build Direction Perpendicular to Applied Force Direction, Raster Angles= (45,-45)	
						Yield Strength (MPa)	Compressive Modulus (MPa)	Yield Strength (MPa)	Compressive Modulus (MPa)	Yield Strength (MPa)	Compressive Modulus (MPa)
Solid	-	-	35.396	43	43.06	97.009	1111.98	-	-	-	-
sp1	2.54	1.02	20.156	29	23.78	30.68	680.03	18.27	511.79	12.89	338.39
sp2	2.54	1.52	21.631	31	25.74	33.78	710.98	22.33	574.40	15.92	417.61
sp3	2.54	2.03	23.106	34	27.60	36.81	750.01	28.13	661.20	19.51	483.80
sp4	2.54	2.54	24.417	36	29.31	38.81	784.002	31.71	718.77	23.30	541.99
sp5	3.81	1.02	16.879	28	19.78	22.68	557.99	15.03	431.40	11.16	293.78
sp6	3.81	1.52	18.845	29	22.18	27.09	605.98	18.75	491.28	14.68	382.59
sp7	3.81	2.03	20.484	31	24.44	30.19	649.96	23.44	572.40	18.06	452.98
sp8	3.81	2.54	22.123	34	26.45	32.40	692.99	26.13	629.62	21.09	515.38
sp9	5.08	1.02	15.240	26	17.72	18.89	482.01	10.82	368.38	9.37	257.38
sp10	5.08	1.52	17.370	29	20.24	23.09	549.99	13.58	446.57	13.30	346.39
sp11	5.08	2.03	19.173	30	22.57	26.20	587.01	16.89	523.79	16.34	431.61
sp12	5.08	2.54	20.812	33	24.78	27.78	619.97	18.96	589.22	19.44	492.14
sp13	6.35	1.02	14.093	27	16.16	15.30	430.99	8.13	342.60	8.27	277.37
sp14	6.35	1.52	16.223	28	18.91	17.99	482.01	10.61	416.78	11.72	368.18
sp15	6.35	2.03	18.190	31	21.49	20.68	533.03	13.44	485.18	15.65	440.02
sp16	6.35	2.54	20.156	32	23.84	22.89	593.01	16.47	535.79	18.68	501.11

Table 4 Surface roughness comparison for the parts in Figure 6 fabricated in different build directions and raster orientations.

Build Direction and Raster Orientation	Surface Roughness R_a (µm)		Surface Roughness R_m (µm)	
	x	y	x	y
Build direction is z-vertical; Raster angles = (45°,-45°)	21.69	N/A	101.34	N/A
Build direction is y-vertical; Raster angles = (0°,90°)	0.43	19.21	4.03	80.92
Build direction is y-vertical; Raster angles = (45°,-45°)	0.43	19.21	4.03	80.92

4. Conclusion

We have investigated sparse-build rapid tooling using the FDM process by performing compression and flexure tests with coupons having ULTEM 9085 as the material and varying air gap (sparse spacing), wall thickness, and cap thickness. The strength/mass ratio and modulus/mass ratio were obtained and compared among the various coupons fabricated with the sparse and sparse-double dense build styles of Stratasys' Fortus machine as well as with solid coupons. It was found that the sparse-double dense coupons have much higher strength-to-mass and modulus-to-mass ratios than the sparse (no double dense) coupons in both compression and flexure tests. Compared to solid coupons, the sparse-double dense coupons have lower compressive strength/mass ratio but higher compressive modulus/mass ratio, flexural strength/mass ratio, and flexural modulus/mass ratio. In terms of sparse-build parameters, it was found that air gap is the most important parameter in compression properties: the compressive strength is higher for a smaller air gap; cap thickness is the most important parameter in flexure properties: the flexural strength is higher for a larger cap thickness. Also, wall thickness has a positive effect and cap thickness has a negative effect on compression properties; air gap has a positive effect but there is no clear trend for wall thickness on flexure properties.

The build direction and raster orientation affect the compressive properties and surface roughness of a part built by the FDM process. The compressive strength and modulus of a coupon are higher when the applied force is parallel to the build direction (i.e., normal to the build layer plane) than when the applied force is perpendicular to the build direction (i.e., parallel to the build layer plane). When the applied force is perpendicular to the build direction, the strength is higher when the angles between the raster path and the applied force are $(0^o, 90^o)$, in comparison to when the angles between the raster path and the applied force are $(45^o, -45^o)$. Build direction also affects surface roughness, which is mainly due to the stair-step effect for a curved surface and depends on the maximum angle between the curved surface and the build direction: the smaller the angle, the smoother the surface.

Acknowledgement

References

[1] ASTM. ASTM F2792–10 standard terminology for additive manufacturing technologies

[2] Novakova-Marcincinova, L. and Kuric, I., "Basic and advanced materials for fused deposition modeling rapid prototyping technology," Journal of Manufacutring and Industrial Engineering, Vol. 11, No. 1, pp. 24-27, 2012.

[3] Crump, S.S., "Fused Deposition Modeling (FDM®): Putting rapid back into prototyping," Proceedings of the Second International Conference on Rapid Prototyping, Dayton, OH, pp. 354-357, 1991.

[4] Sood, A.K., Ohdar, R.K., and Mahapatra, S.S., "Experimental investigation and empirical modeling of FDM process for compressive strength improvement," Journal of Advanced Research, Vol. 3, pp. 81–90, 2012.

[5] Iyibilgin, O., Yigit, C., and Leu, M.C., "Experimental investigation of different cellular lattice structures manufactured by fused deposition modeling," Proceedings of Solid Freeform Fabrication Symposium, Austin, TX, 2013, pp. 895-907, 2012.

[6] Montero, M., Roundy, S., Odell, D., Ahn, S.H., and Wright, P.K., "Material characterization of fused deposition modeling (FDM) ABS by designed experiments," Proceedings of Rapid Prototyping and Manufacturing Conference, SME, 2001.

[7] Lee, C.S., Kim, S.G., Kim, H. J., and Ahn, S.H., "Measurement of anisotropic compressive strength of rapid prototyping parts," Journal of Materials Processing Technology, Vol. 187, pp. 627-630, 2007.

[8] Levasseur, A., Ploeg, H.L., and Petit, Y., "Comparison of the influences of structural characteristics on bulk mechanical behavior: experimental study using a bone surrogate," Journal of Medical and Biological Engineering and Computing, Vol. 50, No. 1, pp. 61-67, 2012.

[9] FDM materials: http://www.funtech.com/FDM-Materials, 2014.

[10] Stratasys: http://www.fortus.com/Products/~/media/Fortus/Files/PDFs/MS-ABS-M30-FORTUS.ashx, 2014.

[11] Guo, N. and Leu, M.C., "Additive manufacturing technology, applications and research needs," Journal of Frontiers of Mechanical Engineering, Vol. 8, No. 3, pp. 215-243, 2013.